13991

Bearing Friction Torque in Bolted Joints

Sayed A. Nassar, G. C. Barber, Dajun Zuo
Fastening and Joining Research Institute
Mechanical Engineering Department
Oakland University, Rochester, Michigan 48309 U.S.A.

Abstract: In this paper, formulas are developed for the calculation of the effective radius of the bearing friction forces on the rotating contact surface in threaded fasteners. These formulas provide a more accurate estimation of the underhead bearing friction torque component in threaded fastener applications. This enhances the reliability, safety, and the quality of bolted assemblies, especially in critical applications. It is well known that the torque-tension correlation in threaded fasteners, and the resulting joint clamping force, is highly sensitive to friction torque components: under the turning head and between threads. This analysis focuses on the bearing friction torque component under the turning head of a threaded fastener. Further, it analyzes the error contained in the current practice when an approximate value, equal to the mean contact surface radius, is used instead of the actual bearing radius. The new formulas for the bearing friction radius are developed for a mathematical model of a bolted joint using four different scenarios of the contact pressure distribution under the rotating fastener head or nut. The effect of the radially varying sliding speed over the rotating contact surface is analyzed and compared with a constant friction coefficient scenario. Numerical results and error analysis are presented in terms of a single non-dimensional variable; namely, the radii ratio between the outside and the inside bearing area.

Keywords: Bolted joints, threaded fasteners, underhead friction, bearing friction, underhead friction torque, bearing radius, torque-tension relationship, thread friction, torque, pitch torque, fastener underhead pressure.

Correspondence regarding this paper should be directed to Sayed A. Nassar, Mechanical Engineering Department, Oakland University, Rochester, MI 48309.

Nomenclature:

D	nominal diameter of the fastener
r_b	effective radius of the contact area under the turning head or nut of the fastener
r_t	effective thread contact radius
F	fastener tension
P	underhead contact pressure
r_m	mean of the contact area under the turning fastener head (or nut)
γ	ratio of the maximum to minimum contact radii
a	exponent
P_{max}	maximum contact pressure

Report Documentation Page

Form Approved
OMB No. 0704-0188

1. REPORT DATE
12 FEB 2004

2. REPORT TYPE

3. DATES COVERED
-

4. TITLE AND SUBTITLE
Bearing Friction Torque in Bolted Joints

5a. CONTRACT NUMBER
DAAE07-03-C-L110

5b. GRANT NUMBER

5c. PROGRAM ELEMENT NUMBER

6. AUTHOR(S)
SAYED NASSAR; G BARBER; DAJUN ZUO

5d. PROJECT NUMBER

5e. TASK NUMBER

5f. WORK UNIT NUMBER

7. PERFORMING ORGANIZATION NAME(S) AND ADDRESS(ES)
FASTENING AND JOINING RESEARCH INSTITUTE,MECHANICAL ENGINEERING DEPARTMENT,OAKLAND UNIVERSITY,ROCHESTER,MI,48309

8. PERFORMING ORGANIZATION REPORT NUMBER

9. SPONSORING/MONITORING AGENCY NAME(S) AND ADDRESS(ES)

10. SPONSOR/MONITOR'S ACRONYM(S)

11. SPONSOR/MONITOR'S REPORT NUMBER(S)

12. DISTRIBUTION/AVAILABILITY STATEMENT
Approved for public release; distribution unlimited

13. SUPPLEMENTARY NOTES

14. ABSTRACT
In this paper, formulas are developed for the calculation of the effective radius of the bearing friction forces on the rotating contact surface in threaded fasteners. These formulas provide a more accurate estimation of the underhead bearing friction torque component in threaded fastener applications. This enhances the reliability, safety, and the quality of bolted assemblies, especially in critical applications. It is well known that the torque-tension correlation in threaded fasteners, and the resulting joint clamping force, is highly sensitive to friction torque components: under the turning head and between threads. This analysis focuses on the bearing friction torque component under the turning head of a threaded fastener. Further, it analyzes the error contained in the current practice when an approximate value, equal to the mean contact surface radius, is used instead of the actual bearing radius. The new formulas for the bearing friction radius are developed for a mathematical model of a bolted joint using four different scenarios of the contact pressure distribution under the rotating fastener head or nut. The effect of the radially varying sliding speed over the rotating contact surface is analyzed and compared with a constant friction coefficient scenario. Numerical results and error analysis are presented in terms of a single non-dimensional variable; namely, the radii ratio between the outside and the inside bearing area.

15. SUBJECT TERMS

16. SECURITY CLASSIFICATION OF:			17. LIMITATION OF ABSTRACT	18. NUMBER OF PAGES	19a. NAME OF RESPONSIBLE PERSON
a. REPORT	b. ABSTRACT	c. THIS PAGE		**16**	
unclassified	**unclassified**	**unclassified**			

P_{min} minimum contact pressure
r radial position from the fastener center
μ_b coefficient of friction between the turning head/nut and the bearing surface
μ_t coefficient of friction between male and female threads
β half of the thread profile angle
p thread pitch

1 Introduction

The safety, reliability, and the quality of bolted assemblies are significantly affected by the level and by the stability of the fastener tension which is most commonly achieved by either turning of the head or the nut of the threaded fastener. In most applications, a very high percentage of the input torquing power is consumed in overcoming the combined effect of two frictional torque components. The first is the bearing friction torque component which must overcome the friction between turning head or nut and the surface of the bolted assembly. The second is the thread friction component that goes into overcoming thread friction. After overcoming bearing and thread friction, only a much smaller percentage of the input torquing power is the useful part that creates the fastener elongation and tension, and simultaneously produce the clamping force in the joint. The torque-tension relationship in threaded fastener applications is highly sensitive to friction torque variations. Moderate friction torque variations, which are particularly common in industrial applications, have significant impact on both the level and the stability of the clamping force in bolted assemblies [1-3]. It should be pointed out that the frictional torque components [4] depend on the bearing and thread friction coefficients, thread and fastener geometry, and on the fastener tension [4].

Inaccuracies in determining the friction torque components result in one of two consequences: either an overestimation or an underestimation of the torque components. On the one hand, an overestimation of the frictional torque components will lead to the underestimation of the actual fastener tension and clamp force in the joint. This may lead to material failure due to overstressing. On the other hand, an underestimation of the friction torque components results in achieving lower fastener tension and clamp force in the joint. That has the potential to cause unexpected fastener loosening, joint separation, leakage, rattle, and fatigue failure.

The torque tension relationship is often simplified by using a tabulated constant known as the nut factor. Juvinall [3] provides an approximate value of 0.2 for the nut factor, but cautions against using it for critical joints without providing guidance as to establish a more reliable yet practical torque-tension relationship. Bickford [1] provides some mean values of the nut factor for various combinations of joint materials and surface conditions. However, the scatter in the nut factor is too great to render it reliable, particularly in critical joints.

In the absence of prevailing torque, and neglecting the three dimensional effect of the helix angle of the thread profile, Motosh [5] provided a more accurate torque-tension relationship for a threaded fastener as follows

$$T = [\frac{p}{2\pi} + \frac{\mu_t r_t}{\cos\beta} + \mu_b r_b]F \quad , \tag{1}$$

where, T is the input tightening torque applied to the fastener head of nut, F is the fastener tension, p is the thread pitch, μ_t is the coefficient of friction between male and female threads, μ_b is the coefficient of friction between the bearing surfaces under the turning fastener head or nut, r_t is an effective contact radius between threads, r_b is an effective bearing radius of the bearing contact area under the turning head or nut, and β is half of the thread profile angle which is 30° for standard UN and ISO threads.

Equation (1) may be expressed as

$$T = T_p + T_t + T_b \quad , \tag{2}$$

where T_p is the pitch torque component that creates the fastener tension and joint clamping force F. The pitch torque component is given by

$$T_p = \frac{p}{2\pi}F , \tag{3a}$$

T_t is the torque component that overcomes the friction between male and female threads, and is given by

$$T_t = \frac{\mu_t r_t}{\cos\beta}F , \tag{3b}$$

and T_b is the bearing friction torque component that overcomes friction between the turning fastener head or nut and the clamped joint surface, and is given by

$$T_b = \mu_b r_b F . \tag{3c}$$

In order to calculate the bearing friction torque component, Shoberg [6] and others use the mean radius of the contact area in equation (3c), in place of an actual effective radius r_b. In this paper, however, new formulas are introduced for the bearing radius r_b in order to be used for the calculation of the bearing friction torque component T_b according to equation (3c), for each of the four models of the underhead pressure distribution. Additionally, the new formulas take into account the effect of the varying sliding speed.

Neglecting the hole clearance, the mean contact radius is given by

$$r_m = \frac{(\gamma+1)D}{2} \qquad , \tag{4}$$

where D is nominal size of the fastener and γ is the ratio of the outside to inside radii of the contact area as shown on Figure (1). In addition, a constant coefficient of friction between the sliding surfaces is normally used for μ_b in order to calculate the bearing friction torque component according to Equation (3c).

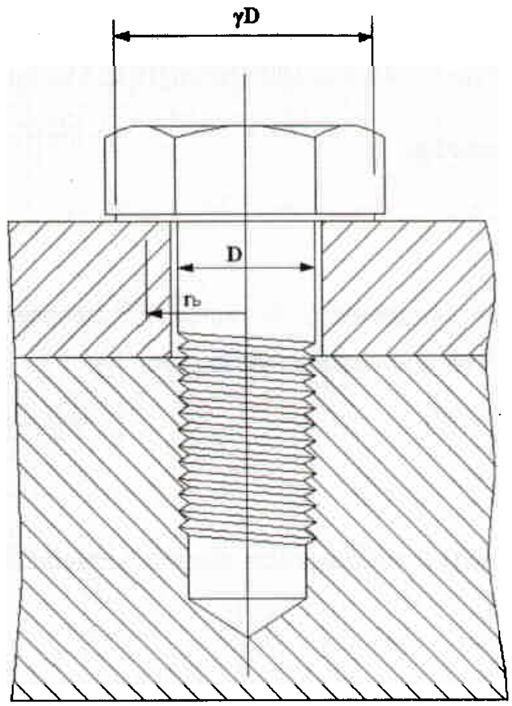

Figure 1 *Bolted Joint Model*

The formulas are valid for various sizes of standard hexagonal or flange head or nuts. Finally, the error introduced by using the mean radius r_m in order to determine the torque component T_b instead of using the exact value of r_b in equation (3c), is discussed in this paper.

2 Static Equilibrium Considerations

At the end of the tightening process of a threaded fastener, the relationship between the fastener tension F and the underhead contact pressure p is given by

$$F = \int_{\substack{contact \\ area}} PdA = 2\pi \int_{r_i}^{r_i} rPdr . \qquad (5)$$

In general, the contact pressure p is not uniform.

The amount of torque consumed to overcome the bearing friction between the head/nut and the clamped surface is

$$T_b = \int (\mu_b PdA) r \qquad (6)$$

$$T_b = 2\pi \int_{r_i}^{r_i} P\mu_b r^2 dr \quad , \qquad (7)$$

where μ_b generally varies over the fastener underhead contact area due to the varying sliding speed of various contact points. During the tightening of a threaded fastener by turning its head (or nut) at a known angular speed, the linear speed of various sliding points on the contact surface will vary linearly with the radial location from the center of the fastener. A more accurate calculation of the bearing friction torque component will have to take the variation in the friction coefficient μ_b.

One way to incorporate the effect of the varying sliding speed on the bearing friction coefficient [7] is by using

$$\mu_b = \mu_i \left(\frac{r_i}{r}\right)^{0.1} \quad , \qquad (8)$$

where μ_i is μ_b at $r = r_i$. Substituting from equation (8) into equation (7), the torque component T_b is

$$T_b = 2\pi r_i^{0.1} \mu_i \int_{r_i}^{r_i} r^{1.9} Pdr \qquad (9)$$

On the other hand, an average value of μ_b would seem appropriate to use in equation (3c). Then

$$T_b = \mu_{average} r_b F \quad , \qquad (10)$$

where

$$\mu_{average} = \frac{\int_{r_i}^{\gamma r_i} \mu_b dA}{\int_{r_i}^{\gamma r_i} dA}$$

$$\mu_{average} = \mu_i \left[\frac{1.052(\gamma^{1.9} - 1)}{\gamma^2 - 1} \right]. \tag{11}$$

Finally, the substitution of equations (5) and (1) into equation (10) and comparing the resulting expression for T_b with that given by equation (9) yields a mathematical expression for the effective bearing friction radius r_b as follows

$$r_b = \frac{0.95(\gamma^2 - 1) r_i^{0.1}}{(\gamma^{1.9} - 1)} * \frac{\int_{r_i}^{\gamma r_i} r^{1.9} P dr}{\int_{r_i}^{\gamma r_i} r P dr} \tag{12}$$

Had the sliding speed effect on the coefficient of friction been neglected [1], the expression for r_b would have been

$$r_b = \frac{\int_{r_i}^{\gamma r_i} r^2 P dr}{\int_{r_i}^{\gamma r_i} r P dr} \qquad (\text{constant } \mu_b)\,. \tag{13}$$

The percent error introduced by using the mean contact radius r_m in place of r_b in equations (12) and (13) is determined by

$$Error(\%) = \left(\frac{r_b - r_m}{r_b} \right)(100) = \left(1 - \frac{r_m}{r_b} \right)(100) \tag{14}$$

where r_m, r_b are determined by equations (4), (12), and (13) for various scenarios of underhead contact pressure distribution.

3 Effect of Underhead Pressure Distribution

Four scenarios of underhead pressure distribution are presented in this paper. A uniform pressure distribution simulates the use of a strong steel bolt and nut to clamp on a much weaker clamping surface such as plastic surfaces or soft washers. Other pressure distributions considered would simulate contact stress concentration at the edge of the fastener hole, or may by contrast reflect the zero pressure conditions at minimum or maximum radii of the contact area.

Model 1: Uniform Underhead Pressure

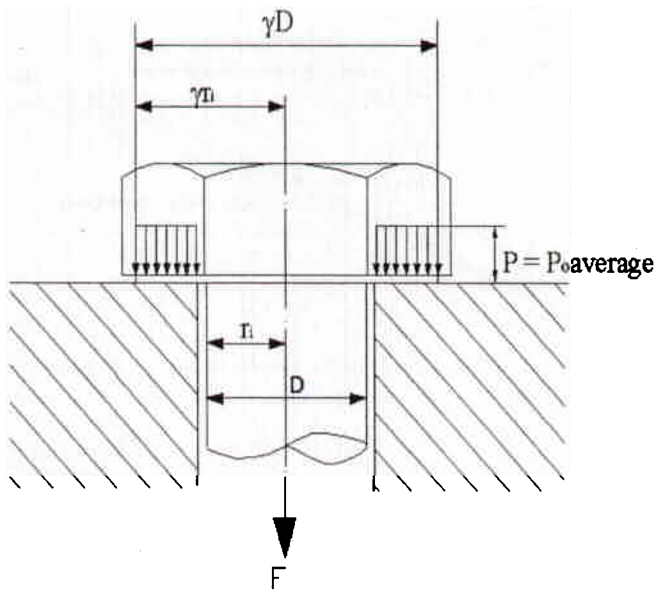

Figure 2 *Constant Underhead Pressure*

If the contact pressure p is uniform as shown in Figure 2 its value would be given by

$$P = \frac{F}{\pi(\gamma^2 - 1)r_i} \, . \tag{15}$$

Substituting the constant pressure equation (15) into equation (12) yields

$$r_b = \frac{0.656(\gamma^{2.9} - 1)r_i}{(\gamma^{1.9} - 1)} \, . \tag{16}$$

From equations (16) and (4), the ratio r_m/r_b is given by

$$\frac{r_m}{r_b} = \frac{(\gamma^{1.9} - 1)(\gamma + 1)}{1.312(\gamma^{2.9} - 1)} \, . \tag{17}$$

The percent error is determined according to equation (14) and shown on Figure 3.

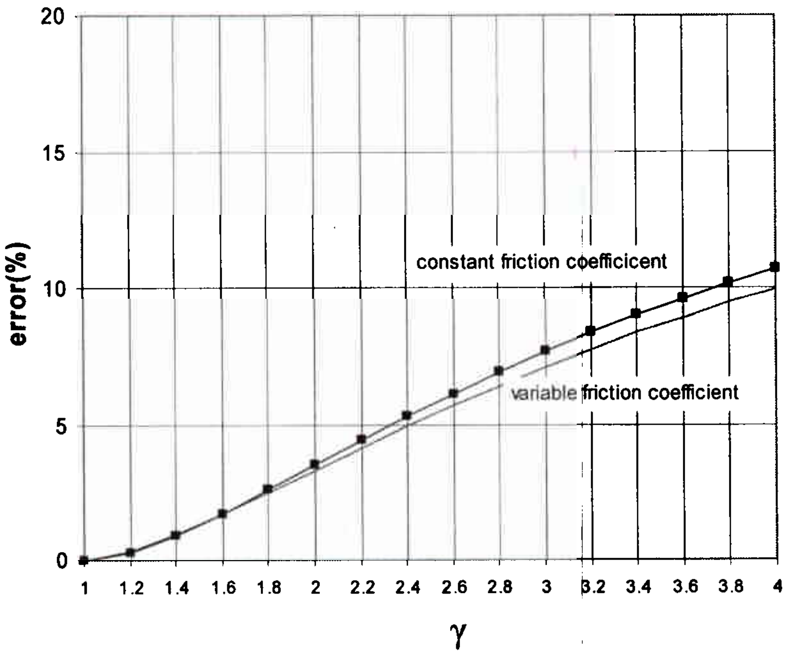

Figure 3 *Percent error : Constant Underhead Pressure Distribution Model*

Model 2 Sinusoidal Underhead Pressure

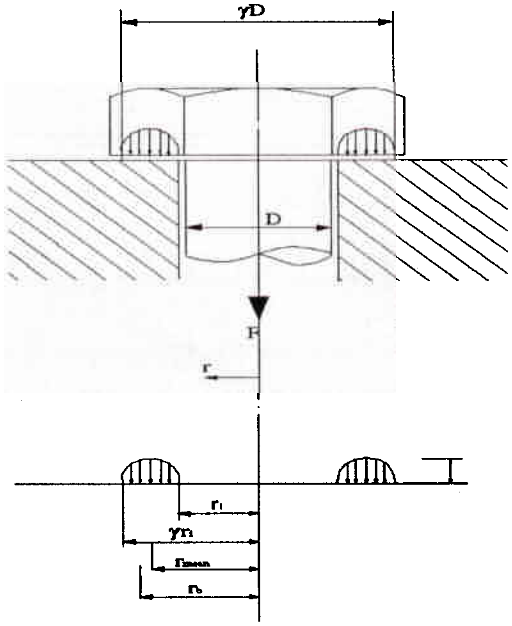

Figure 4 Sinusoidal Underhead Pressure

The sinusoidal contact pressures shown in Figure (4) may be expressed as

$$P = P_{max} \sin\left[\frac{\pi(r - r_i)}{r_i(\gamma - 1)}\right]. \tag{18}$$

The peak pressure P_{max} is obtained by substituting equation (18) into the static equilibrium equation (5), which yields

$$P_{max} = \frac{F}{2r_i^2(\gamma^2 - 1)}. \tag{19}$$

Equations (4), (12), (18), and (19) give the effective bearing friction radius as follows

$$r_b = \frac{0.95(\gamma^2 - 1)r_i^{0.1}}{\gamma^{1.9} - 1} \bullet \frac{\int_{r_i}^{\gamma r_i} r^{1.9} \sin[\frac{\pi(r - r_i)}{r_i(\gamma - 1)}]dr}{\int_{r_i}^{\gamma r_i} r \sin[\frac{\pi(r - r_i)}{r_i(\gamma - 1)}]dr} \tag{20}$$

The integrals on the right hand side of the equation yield long expressions that are naturally dependent on the inside radius of contact area r_i, which equals the nominal radius of the fastener, approximately. However, the ratio r_m/r_b is independent of the fastener radius r_i by itself, and depends only on the radii ratio γ. The percent error is calculated according to equation (14), and is depicted by Figure 5.

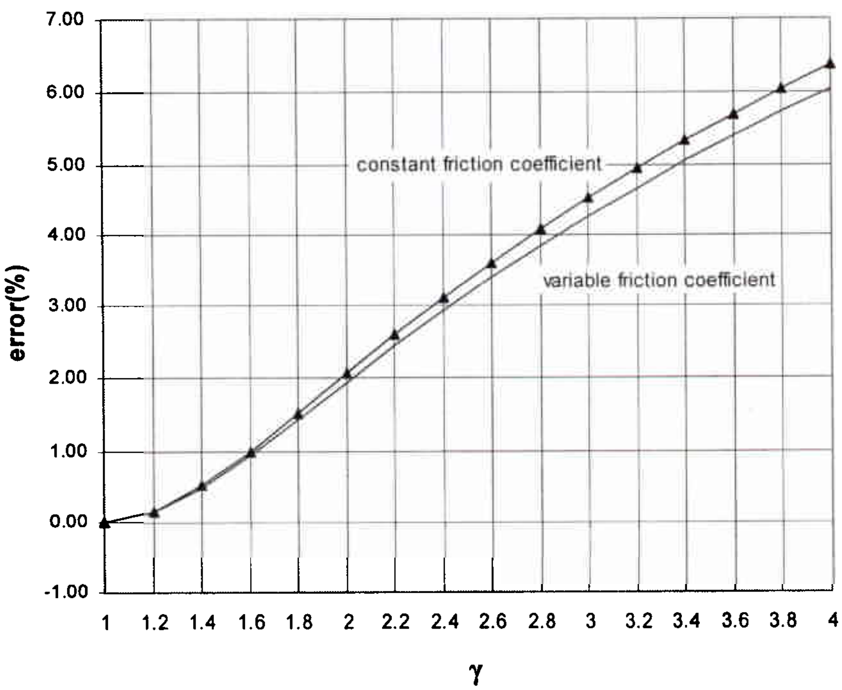

Figure 5 *Percent error : Sinusoidal Underhead Pressure Distribution Model*

Model 3 Exponentially Decreasing Pressure

Figure 6 shows a pressure model in which the underhead pressure decreases exponentially from P_{max} at the edge of the hole to P_{min} at the outside radius of the contact area under the turning fastener head or nut. This pressure distribution is given by

$$P = P_{\max} e^{-ar'} \qquad [0 \le r' \le \gamma r_i - r_i], \tag{21}$$

where *a* is a positive exponent, and *r'* is radial distance measured from the edge of the hole.

It must be noted that the relation between the ratio P_{min}/P_{max} and the exponent *a* is given by

$$\frac{P_{\min}}{P_{\max}} = e^{-ar_i(\gamma-1)}. \tag{22}$$

The exponent a is obtained from equation (22) for various ratios of P_{min}/P_{max} as follows

$$a = \frac{\ln \frac{P_{max}}{P_{min}}}{r_i(\gamma - 1)} \tag{23}$$

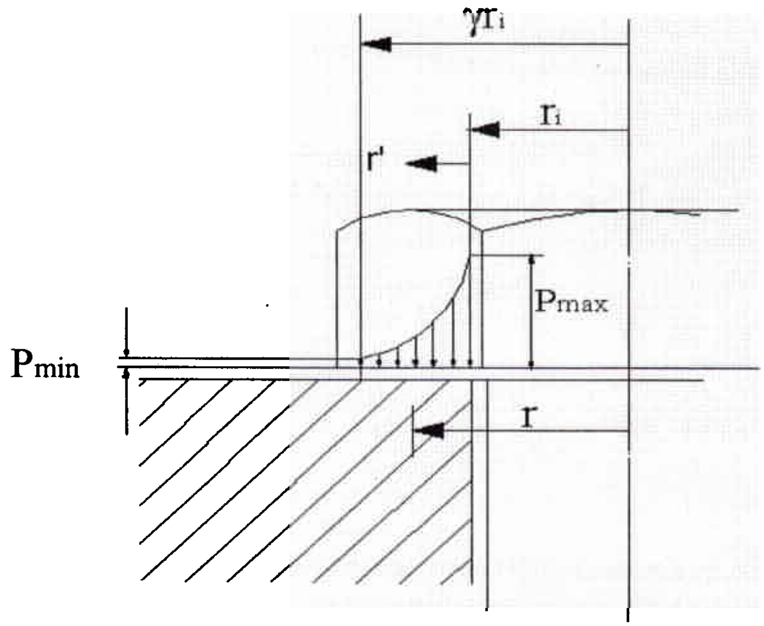

Figure 6 *Percent Error: Exponentially Varying Underhead Pressure*

The selected range for the pressure ratio is $0.01 \le P_{min} / P_{max} \le 1$. The low limit of the selected range simulates a rapid exponential decrease of the contact pressure, in which the high limit simulates the case of uniform contact pressure (Model 1). Combining equations (4), (12), (22), and (23) yields

$$r_b = \frac{0.95(\gamma^2 - 1)r_i^{0.1}}{\gamma^{1.9} - 1} * \frac{\int_{r_i}^{\gamma r_i} r^{1.9} e^{-a(r-r_i)} dr}{\int_{r_i}^{\gamma r_i} r e^{-a(r-r_i)} dr}. \tag{24}$$

Equation (24) is numerically integrated for various ratios of P_{min}/P_{max}, and the results of r_b are once again compared with the mean radius $r_m = \frac{(\gamma+1)r_i}{2}$. The percent error in the beraing friction torque component that results from using r_m is shown in Figure 7.

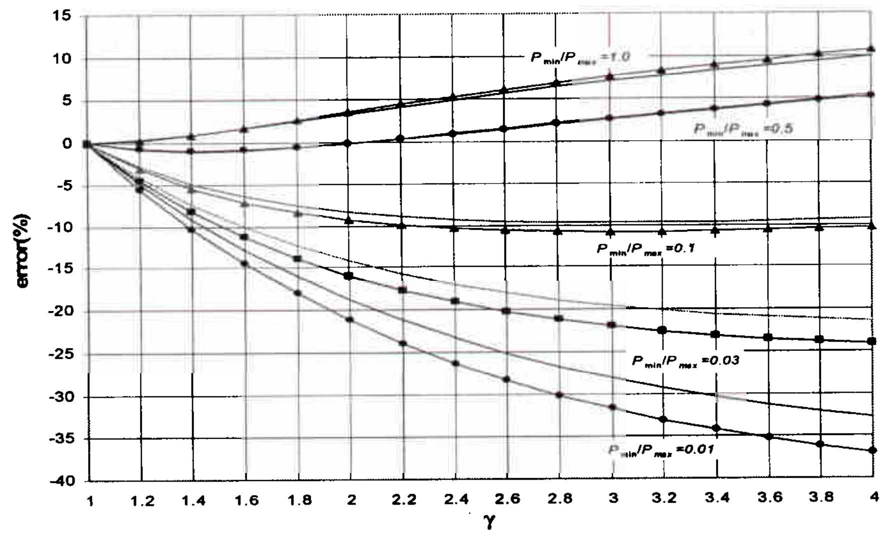

Figure 7 *Percent error : Exponential Underhead Pressure Distribution Model (curves with and without dots represent results for uniform vs. radially varying friction, respectively)*

Model 4 Linearly Decreasing Pressure

The final scenario considered in this paper depicts a contact pressure distribution that linearly from P_{max} at the edge of the hole to zero at the outer radius of the contact surface, as shown in Figure 8. The contact pressure at any radial position r is given by

$$P = \frac{(\gamma r_i - r)}{r_i(\gamma - 1)} P_{max} \, . \qquad (25)$$

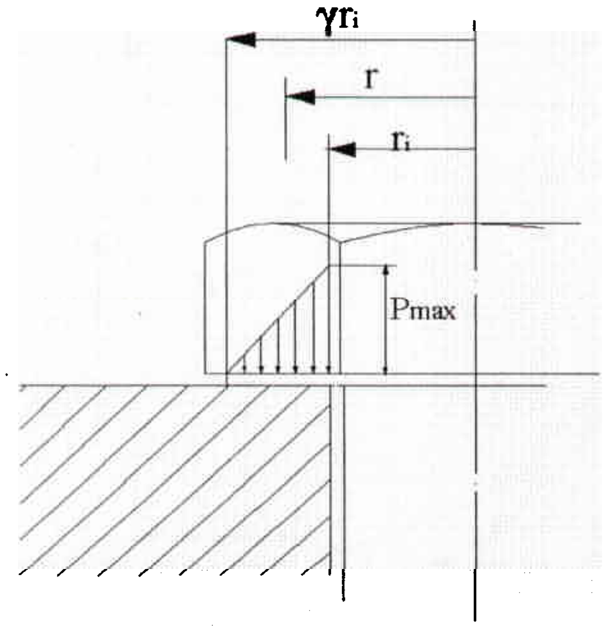

Figure 8 *Linearly Decreasing Underhead Pressure*

The maximum contact pressure P_{max} is determined by substituting equation (25) into equation (5). The effective bearing radius is obtained by using equation (12) and (25) as follows

$$r_b = \frac{0.95 r_i(\gamma^2 - 1)}{\gamma^{1.9} - 1} * \frac{6\gamma^{3.9} - 23.4\gamma + 17.4}{11.31\gamma^3 - 33.93\gamma + 22.62}, \qquad (26)$$

and the ratio r_m/r_b becomes

$$\frac{r_m}{r_b} = \frac{(\gamma^{1.9} - 1)(11.31\gamma^2 - 33.93\gamma + 22.62)}{1.90(\gamma - 1)(6\gamma^{3.9} - 23.4\gamma + 17.4)}. \qquad (27)$$

Had the effect of the sliding speed on the bearing friction coefficient been neglected, this ratio would be given by

$$\frac{r_m}{r_b} = \frac{\gamma^2 + 3\gamma + 2}{\gamma^2 + 2\gamma + 3}. \qquad \text{(Constant friction)} \qquad (28)$$

Numerical results for this model of pressure distribution are shown on Figure 9.

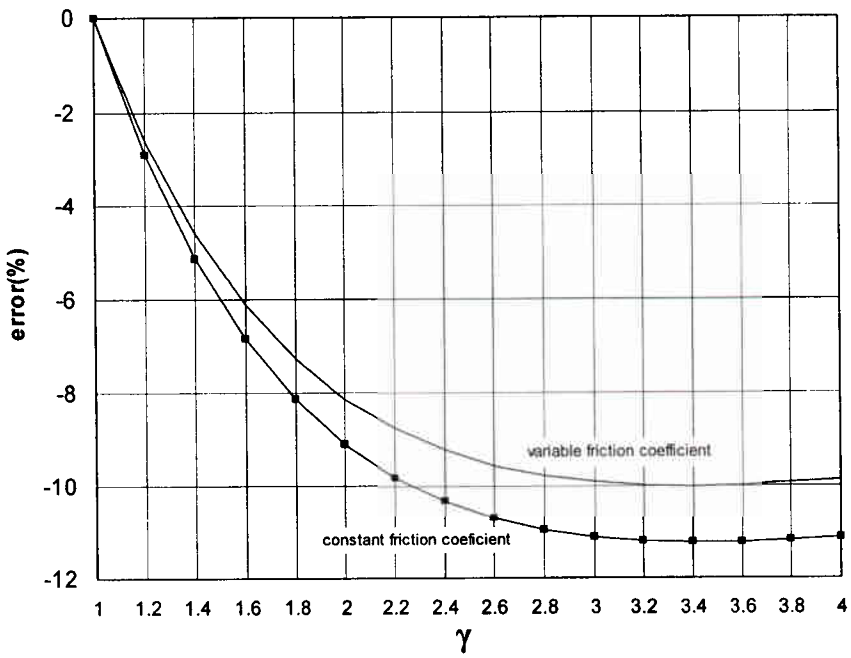

Figure 9 *Linearly Varying Underhead Pressure Distribution Model*

4 Results and Discussion

For the four scenarios of the contact pressure distribution, expressions for the effective radius r_b of the bearing friction forces are provided by equations (16), (20), (24), and (26). By comparing the effective radius r_b to the geometric mean radius r_m of the bearing area, the percent error is calculated according to equation (14). This error is introduced by using the latter radius (r_m) in order to determine the bearing friction torque component T_b given by equation (3c). On the one hand, a positive percent error indicates an underestimation of the bearing friction torque component when the mean radius r_m is used instead of r_b. This will result in a lower torque-tension ratio for the fastener and it will result in a lower clamping force in a bolted joint. On the other hand, a negative error indicates an overestimation of the bearing friction that ultimately leads to higher torque-tension ratio in the fastener, and to a higher clamping force in the joint.

Figures 3, 5, 7, and 9 show the percent error in the bearing friction torque component, that results from using r_m as an approximation for r_b. The error is expressed in terms of a single non-dimensional variable γ, which describes the ratio of the outside radius to inside radius of the bearing area. The ratio γ is approximately equal to 1.5 for standard hexagonal fastener heads and nuts; it is smaller for socket head fasteners and it takes a value between 2 and 3 for most flanged head and flanged nut applications.

For the case of a constant underhead pressure, the percent error introduced by using r_m instead of r_b, in the calculation of the bearing friction torque component, is shown on

Figure 3. For most standard threaded fasteners, the error is less than 5% and the effect of taking the variation in sliding speed into account is insignificant. Similar results are shown in Figure 5 for the sinusoidal pressure distribution scenario.

As for the exponential underhead pressure distribution, Figure 7 shows that the percent error is significantly influenced by two additional factors; namely, by the rate at which the underhead pressure is varied, and by whether the friction variation due to the variable sliding speed has been taken into account. For a given bearing area, a small P_{min}/P_{max}, produces a significantly larger percent error. For the most commonly used fastener applications γ falls between 1.5 and 3. As it can be seen on Figure 7, the magnitude of the error in such fastener applications is as high as 33%, when P_{min}/P_{max} ratio of one percent and a uniform bearing friction model is used. The same figure shows that the error drops to 28% by considering a variable bearing friction model, in which the effect of a radially varying sliding speed on the bearing friction coefficient has been taken into account.

Figure 9 provides the error analysis for the case of a linearly decreasing fastener underhead pressure model. The magnitude of the maximum error for most common fastener applications about 10% and the effect of the variation in bearing friction is insignificant. Further, the error results of this model are closest to those on Figure 7, with a P_{min}/P_{max} equal to 0.1.

5 Conclusions

The new formulas developed in this paper provide a more accurate calculation of the fastener underhead bearing friction torque component. This will enhance the quality, safety and the reliability of many mechanical and structural components. The use of the mean radius of the contact area should be replaced by using formulas developed in this paper, for determining the actual bearing friction radius. Numerical results suggest that the improved accuracy is more noticeable for applications in which the ratio γ of the contact radii is higher. Similarly, the effect of the variable sliding speed on the bearing friction torque component increases with increasing the bearing radii ratio γ . Finally, the numerical results show that the modeling of the fastener underhead pressure has a significant effect on the bearing friction torque component and on the overall fastener torque-tension relationship. This has direct impact on the level of the clamping force achieved in the joint when the fastener is initially tightened to a given torque level.

References

1- Bickford, John H., An Introduction to the Design and Analysis of Bolted Joints, third edition, Marcel Dekker, New York, New York, 1997.

2- Bickford, John H., and Nassar, Sayed, Handbook of Bolts and Bolted Joints, Marcel Dekker, New York, New York, 1998.

3- Juvinall, Robert C., and Marshek, Kurt M., Fundamentals of Machine Component Design, , third edition, John Wiley &Sons, New York, New York, 2000.

4- Jiang, Y., Chang, J., and Lee, C., "An Experimental study of torque-tensionr elationship for bolted joints", *International Journal of Materials and Product Technology*, 2000, Vol. 16, No. 4/5, pp. 417-429.

5- Motosh, N, " Development of Design Charts for Bolts Preloaded up to the Plastic Range", ASME Journal of Engineering for Industry, 1976, pp. 849-851.

6- Shoberg, Ralph, Manual for the T3 Torque-Tension-Friction Testing System, GSE Inc., Farmington Hills, MI, 1990.

7- Rabinowicz, Ernest, Friction and Wear of Materials, John Wiley & sons, New York, New York, 1965, pp. 60-61.